J|A|C|S
COMMUNICATIONS

Published on Web 03/07/2007

Reversible Water-Induced Magnetic and Structural Conversion of a Flexible Microporous Ni(II)Fe(III) Ferromagnet

Nobuhiro Yanai, Wakako Kaneko, Ko Yoneda, Masaaki Ohba,* and Susumu Kitagawa*

Department of Synthetic Chemistry and Biological Chemistry, Graduate School of Engineering, Kyoto University, Katsura, Nishikyo-ku, Kyoto 615-8510, Japan

Received December 21, 2006; E-mail: ohba@sbchem.kyoto-u.ac.jp

Flexible and dynamic porous coordination polymers attract much attention as promising functional materials compared with robust polymers.[1] They are regarded as being structurally bistable frameworks and are expected to show not only structural changes but also modulation of their physical properties to achieve multiple functions.[2−4] As for magnetic properties, several magnetic coordination polymers providing an open framework have succeeded in exhibiting reversible guest-induced magnetic conversions by transformation of 0-D,[3e] 1-D,[3c] and 2-D[3b] frameworks or changes of local coordination environments.[3a] Their characterization has been mainly focused on their responses to guest molecules; however, their gas-adsorption abilities have been scarcely evaluated yet. As a next target, we focused on the inherent structural flexibility of 3-D porous magnets, which are expected to show remarkable magnetic and structural conversions in response to gas adsorption/desorption. Such flexibility and porosity are not features inherent in general magnets. These so-called "flexible porous magnets" will exhibit selective accommodation or separation of guest molecules complying with their sizes and shapes, and also specific orientation, alignment, and reaction of the guest molecules in the pores under a strong spontaneous internal magnetic field.

On the other hand, the practical synthesis of porous magnets remains a current issue, because structural demands for high spin density to achieve long-range magnetic ordering conflict with those for porosity.[3,4] One of the rational strategies for porous magnets is based on a framework providing paramagnetic centers located in the sides and corners of the inner pore, where the side and the corner correspond to a connector and a linker for the framework, respectively.[3b] From this viewpoint, the hexacyanometalate anion, $[M(CN)_6]^{n-}$, is a suitable linker, because it gives a relatively long side (ca. 10 Å) for the inner pore and forms monodentate cyanide bridges for effective magnetic interaction[5] and structural flexibility. Here, we prepared a 3-D porous ferromagnet, $[Ni(dipn)]_2[Ni(dipn)(H_2O)][Fe(CN)_6]_2\cdot 11H_2O$ (**1A**)[6] (dipn = *N*,*N*-di(3-aminopropyl)-amine), which shows significant magnetic conversion associated with a reversible gaseous water-induced crystal-to-amorphous-like phase transformation.

Compound **1A** was obtained as dark brown crystals by the reaction of $NiCl_2\cdot 6H_2O$, dipn, and $K_3[Fe(CN)_6]$ in the 3:3:2 mole ratio in DMF−water solution. The dehydrated form, $[Ni(dipn)]_2[Ni(dipn)(H_2O)][Fe(CN)_6]_2\cdot H_2O$ (**1B**), and anhydrous form, $[Ni(dipn)]_3[Fe(CN)_6]_2$ (**1C**), were prepared in vacuum at 298 and 373 K, respectively. Compounds **1A** and **1B** showed two sharp ν_{CN} bands at 2142 and 2120 cm^{-1}, indicating the existence of bridging and terminal cyano groups in the lattice, whereas, ν_{CN} stretching of **1C** gave a broad band around 2050 cm^{-1}, reflecting a disorder of the cyanide bridges by dehydration.

The asymmetric unit of **1A** consists of one $[Fe(CN)_6]^{3-}$ anion, one $[Ni(1)(dipn)]^{2+}$ and one-half $[Ni(2)(dipn)(H_2O)]^{2+}$ cations and 11 water molecules (Supporting Information Figure S1). Three equatorial cyano nitrogen atoms of $[Fe(CN)_6]^{3-}$ (N(1), N(3), and N(6)) coordinate to three adjacent $[Ni(1)(dipn)]^{2+}$ cations, and one axial cyano nitrogen atom (N(2)) coordinates to the axial position of the adjacent $[Ni(2)(dipn)(H_2O)]^{2+}$ cation. In the lattice, the Fe−CN−Ni(1) linkages form a 2-D sheet expanding on the *bc* plane (Figure S2), and the Fe−CN(2)−Ni(2) linkages connect the 2-D sheets along the *a*-axis and construct a 3-D porous framework (Figure 1). The coordinated water in the equatorial position of Ni(2) faces the pore and is incorporated in the inner wall. Only one lattice water that forms bidirectional hydrogen bonds with cyano nitrogen atoms, N(4)* and N(5), has a clearly determined position (O(2)···N(4)* = 2.890 Å, O(2)···N(5) = 3.007 Å, *: symmetry operation ($^1/_2 - x$, $-^1/_2 + y$, $1 - z$)). The other lattice water molecules reside in a disorderly manner in the pore. Rectangular channels are constructed along the [001] direction with estimated gate size of 3.5 × 4.3 $Å^2$ with the coordinated water or 3.5 × 8.7 $Å^2$ without water. The solvent-accessible void in the framework is estimated to be 29.0% by PLATON[7] in the absence of all water molecules.

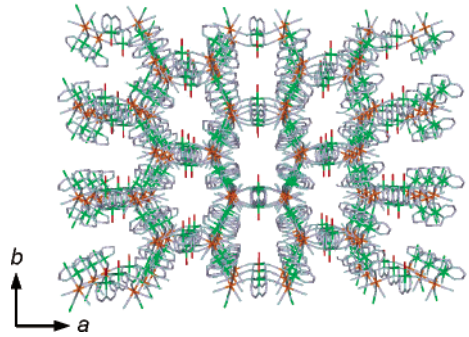

Figure 1. 1-D channel structure of **1A** along the *c*-axis. Lattice water molecules are omitted. Atoms shown are Ni (green), Fe (orange), O (red).

TG−DTA results of **1A** indicated that all the water molecules were removed by 423 K and the framework decomposed above 453 K (Figure S3). Under vacuum at 298 K, **1A** lost 10 water molecules per formula unit, converting to **1B** (Figure S4). Two residual water molecules of **1B** can be assigned to coordinated and hydrogen-bonded ones by structural and TG−DTA results.

A temperature-dependent XRPD investigation under N_2 of **1A** showed that the crystallinity was immediately lost above 313 K, which suggests that the arrangement of the framework was disordered by dehydration (Figure S5). Both the dehydrated form **1B** and the anhydrous form **1C** gave amorphous-like XRPD patterns. Remarkably, the amorphous-like **1B** recovered its crystallinity smoothly on being exposed to gaseous water (100% relative humidity, Figure 2a). The rehydrated form was denoted as **1B′**. TGA results indicated that **1B′** contains 12 water molecules per formula unit, the same as **1A** (Figure S6). On the other hand, **1C** did not recover its crystallinity on being exposed to gaseous water or immersed in water, which suggests the residual lattice water

10.1021/ja069166b CCC: $37.00

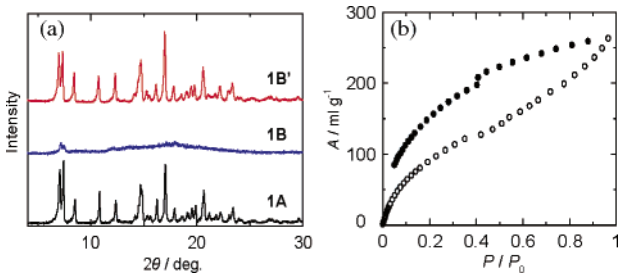

Figure 2. (a) The XRPD patterns of the original form **1A**, the dehydrated form **1B**, and the rehydrated form **1B′**. (b) Water sorption isotherms for **1B** at 298 K. Adsorption and desorption are indicated by open and filled circles, respectively. The ratio of gas pressure to saturation pressure, P/P_0, was obtained with $P_0 = 23.75$ mmHg.

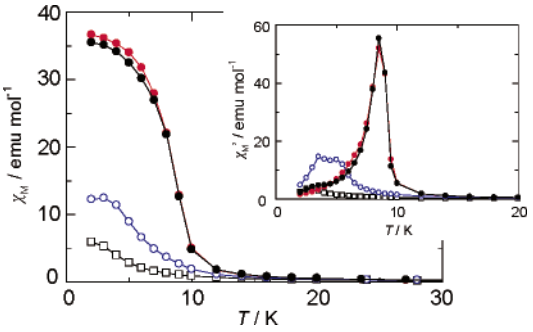

Figure 3. Temperature dependences of χ_M measured under an applied dc field of 500 Oe for **1A** (black circle), **1B** (open circle), **1B′** (red circle), and **1C** (open square). Inset shows the corresponding ac susceptibilities (ac 3 Oe, 100 Hz).

forming bidirectional hydrogen bonds with cyano groups and the coordinated water of Ni(2) play a significant role in the structural recovery. The adsorption isotherms of water on **1B** were measured at 298 K (Figure 2b). Compound **1B** gradually adsorbed water as the relative pressure increased and showed a high uptake of 236 mL/g (9.93 mol/mol) at 21.5 mmHg, indicating that the amorphous-like form **1B** can adsorb water and reconstruct the initial framework without undergoing the dissolution and reprecipitation processes that are often discussed with solution-mediated structural transformations.[1e]

χ_M versus T plots of **1A**, **1B**, **1C**, and **1B′** are shown in Figure 3. The measurements were made in the temperature range 2−50 K because **1A** readily effloresces in a helium atmosphere (under low relative humidity). The χ_M value of **1A** gradually increased upon cooling to 20 K and rapidly increased below 10 K, up to a maximum value of 35.49 emu mol^{-1} (23.83 μ_B) at 2.0 K. This behavior suggests the operation of a ferromagnetic interaction between the adjacent Ni^{II} and low-spin Fe^{III} ions through cyanide bridges because of the strict orthogonality of the magnetic orbitals. A long-range ferromagnetic ordering ($T_c = 8.5$ K) was confirmed by a dM/dT plot, weak-field magnetization measurements, temperature dependences of ac susceptibility, and magnetic hysteresis loop ($\mathbf{H}_c = 350$ Oe) (Figures S7−8). For the dehydrated form **1B**, the curve showed a quite different shape with a small maximum (12.44 emu mol^{-1}) at 3.0 K. The χ_M' versus T plots of **1B** showed two broad peaks around 6.0 and 3.5 K. The magnetic hysteresis loop of **1B** showed an almost paramagnetic behavior with $\mathbf{H}_c = 50$ Oe. These results indicate that the ferromagnetic interaction is weakened and the magnetic domain is moderately fragmented while keeping short-range order by dehydration in **1B**. The dc and ac magnetic results of **1B′** completely reproduced those of the original form **1A**. The magnetic hysteresis loop of **1B′** showed a similar shape to **1A** with larger remnant magnetization, which suggests larger magnetic domains are generated by rehydration. The dehydrated form **1B** and the rehydrated form **1B′** demonstrate that a complete regeneration of the long-range ferromagnetic ordering accompanied the structural recovery. The anhydrous form **1C** did not show ferromagnetic ordering because of the disorder of the bridging structure.

The 3-D porous ferromagnet, $[Ni(dipn)]_2[Ni(dipn)(H_2O)][Fe(CN)_6]_2 \cdot 11H_2O$, demonstrated a remarkable magnetic change associated with the reversible crystal-to-amorphous-like phase transformation triggered by water desorption/adsorption. These results prove that the synthetic strategy based on cyanide-bridged bimetallic assemblies is advantageous for the formation of flexible microporous magnets providing interlocked guest-induced magnetic and structural conversion. The dehydrated form **1B** also adsorbs other guests, such as methanol (Figure S9), so further work will focus on magnetic conversion by organic guests or paramagnetic gases such as O_2 or NO.

Acknowledgment. This work was supported by a Grant-In-Aid for Science Research in a Priority Area "Chemistry of Coordination Space (No. 16074209)" from the Ministry of Education, Science, Sports and Culture, and Core Research for Evolutional Science and Technology (CREST), Japan Science and Technology Corporation (JST), Japan.

Supporting Information Available: Crystal structure for **1A**; TGA, XRPD patterns, and magnetic measurements for each phase; methanol sorption isotherms for **1B**. This material is available free of charge via the Internet at http://pubs.acs.org.

References

(1) (a) Yamada, K.; Tanaka, H.; Yagishita, S.; Adachi, K.; Uemura, T.; Kitagawa, S.; Kawata, S. *Inorg. Chem.* **2006**, *45*, 4322. (b) Kitagawa, S.; Uemura, K. *Chem. Soc. Rev.* **2005**, *34*, 109. (c) Bourrelly, S.; Llewellyn, P. L.; Serre, C.; Millange, F.; Loiseau, T.; Férey, G. *J. Am. Chem. Soc.* **2005**, *127*, 13519. (d) Kitagawa, S.; Kitaura, R.; Noro, S.-i. *Angew. Chem., Int. Ed.* **2004**, *43*, 2334. (e) Rosseinsky, M. J. *Microporous Mesoporous Mater.* **2004**, *73*, 15. (f) Rowsell, J. L. C.; Yaghi, O. M. *Microporous Mesoporous Mater.* **2004**, *73*, 3. (g) Dybtsev, D. N.; Chun, H.; Kim, K. *Angew. Chem., Int. Ed.* **2004**, *43*, 5033. (h) Biradha, K.; Hongo, Y.; Fujita, M. *Angew. Chem., Int. Ed.* **2002**, *41*, 3395. (i) Min, K. S.; Suh, M. P. *Chem.−Eur. J.* **2001**, *7*, 303.

(2) (a) Kepert, C. J. *Chem. Commun.* **2006**, 695. (b) Cui, H.-B.; Takahashi, K.; Okano, Y.; Kobayashi, H.; Wang, Z.; Kobayashi, A. *Angew. Chem., Int. Ed.* **2005**, *44*, 6508. (c) Goodwin, A. L.; Chapman, K. W.; Kepert, C. J. *J. Am. Chem. Soc.* **2005**, *127*, 17980. (d) Niel, V.; Thompson, A. L.; Muñoz, M. C.; Galet, A.; Goeta, A. S. E.; Real, J. A. *Angew. Chem., Int. Ed.* **2003**, *42*, 3760. (e) Halder, G. J.; Kepert, C. J.; Moubaraki, B.; Murray, K. S.; Cashion. J. D. *Science* **2002**, *298*, 1762.

(3) (a) Ohkoshi, S.; Arai, K.; Sato, Y.; Hashimoto, K. *Nat. Mater.* **2004**, *3*, 857. (b) Maspoch, D.; Ruiz-Molina, D.; Wurst, K.; Domingo, N.; Cavallini, M.; Biscarini, F.; Tejada, J.; Rovira, C.; Veciana, J. *Nat. Mater.* **2003**, *2*, 190. (c) Usuki, N.; Ohba, M.; Okawa, H. *Bull. Chem. Soc. Jpn.* **2002**, *75*, 1693. (d) Miyasaka, H.; Ieda, H.; Matsumoto, N.; Re, N.; Crescenzi, R.; Floriani, C. *Inorg. Chem.* **1998**, *37*, 255.

(4) (a) Kurmoo, M.; Kumagai, H.; Chapman, K. W.; Kepert, C. J. *Chem. Commun.* **2005**, 3012. (b) Maspoch, D.; Ruiz-Molina, D.; Veciana, J. *J. Mater. Chem.* **2004**, *14*, 2713. (c) Wang, Z.; Zhang, B.; Fujiwara, B.; Kobayashi, H.; Kurmoo, M. *Chem. Commun.* **2004**, 416. (d) Guillou, N.; Livage, C.; Drillon, M.; Férey, G. *Angew. Chem., Int. Ed.* **2003**, *42*, 5314. (e) Tian, Y.-Q.; Cai, C.-X.; Ren, X.-M.; Duan, C.-Y.; Xu, Y.; Gao, S.; You, X.-Z. *Chem.−Eur. J.* **2003**, *9*, 5673. (f) Moulton, B.; Lu, J.; Hajndl, R.; Hariharan, S.; Zaworotko, M. J. *Angew. Chem., Int. Ed.* **2002**, *41*, 2821. (g) Beauvais, L. G.; Long, J. R. *J. Am. Chem. Soc.* **2002**, *124*, 12096. (h) Larionova, J.; Chavan, S. A.; Yakhmi, J. V.; Frøystein, A. G.; Sletten, J.; Sourisseau, C.; Kahn, O. *Inorg. Chem.* **1997**, *36*, 6374.

(5) Ohba, M.; Ōkawa, H. *Coord. Chem. Rev.* **2000**, *198*, 313.

(6) Ohba, M.; Yamada, M.; Usuki, N.; Ōkawa, H. *Mol. Cryst. Liq. Cryst.* **2002**, *379*, 241. (Details are given in Supporting Information.)

(7) Spek, A. L. *PLATON, A Multipurpose Crystallographic Tool*; Utrecht University: Utrecht, The Netherlands, 2001.

(8) X-ray crystallographic data for **1A** at 243 K ($C_{30}H_{63}N_{21}Fe_2Ni_3O_6$): fw = 1101.76; space group, $C2/c$; $a = 24.044(8)$ Å, $b = 14.343(4)$ Å, $c = 16.688(5)$ Å; $\beta = 100.552(4)$; $V = 5657.6(30)$ Å^3; $Z = 4$; $D_{calcd} = 1.293$ g cm^{-3}. μ(Mo Kα) = 1.533 cm^{-1}; $R = 0.0832$ and $R_w = 0.2048$ (for 6442 reflections, F^2). The position of lattice water molecules could not be accurately determined because of structural disorder. Details are given in Supporting Information.

JA069166B